

## Accepted Manuscript

Effects of methanol on morphology and photoluminescence in solvothermal grown ZnO powders and ZnO on Si

Oscar Marin, Vanessa González, Mónica Tirado, David Comedi

PII: S0167-577X(19)30738-4  
DOI: <https://doi.org/10.1016/j.matlet.2019.05.033>  
Reference: MLBLUE 26146

To appear in: *Materials Letters*

Received Date: 2 March 2019  
Revised Date: 7 May 2019  
Accepted Date: 9 May 2019

Please cite this article as: O. Marin, V. González, M. Tirado, D. Comedi, Effects of methanol on morphology and photoluminescence in solvothermal grown ZnO powders and ZnO on Si, *Materials Letters* (2019), doi: <https://doi.org/10.1016/j.matlet.2019.05.033>

This is a PDF file of an unedited manuscript that has been accepted for publication. As a service to our customers we are providing this early version of the manuscript. The manuscript will undergo copyediting, typesetting, and review of the resulting proof before it is published in its final form. Please note that during the production process errors may be discovered which could affect the content, and all legal disclaimers that apply to the journal pertain.



## Effects of methanol on morphology and photoluminescence in solvothermal grown ZnO powders and ZnO on Si

Oscar Marin\*, Vanessa González, Mónica Tirado and David Comedi\*

INFINOA – CONICET – UNT, Av. Independencia 1800, 4000, Tucumán, Argentina.

\*Corresponding authors: [omarin@herrera.unt.edu.ar](mailto:omarin@herrera.unt.edu.ar); [dcomedi@herrera.unt.edu.ar](mailto:dcomedi@herrera.unt.edu.ar)

### Abstract

ZnO nano and microstructures were obtained by solvothermal synthesis using hexamethylenetetramine (HMTA) as alkaline agent, and water, water/methanol and methanol as solvents. Two types of samples were obtained: A ZnO powder that grew at the bulk solution and ZnO on silicon substrates. The effect of the solvent on the morphology and optical emission was studied, as well as the influence of the growth zone. With increasing methanol content, the morphology changed from nanorods to nanoparticles powders, and from oriented arrangement of nanorods to thin film on silicon substrates. Important changes in photoluminescence induced by the methanol content and depending on the growth zone were also observed.

Keywords: *Solvothermal synthesis; Hexamethylenetetramine; Photoluminescence; ZnO morphology.*

## 1. Introduction

Nanostructures of ZnO (direct band gap of ~3.3 eV) have been drawing increasing attention due to their many potential applications [1]. Particular focus has been directed towards the control of the nanostructure morphology through low temperature growth techniques, such as the solvothermal and chemical bath deposition [2–4]. However, the role of key growth parameters on the morphology has remained elusive. For instance, using ethanolamine family reagents as alkaline additives, spherical ZnO particles were reported [5]. In contrast, HMTA usually leads to ZnO nanorods [3]. Other parameters that may affect the ZnO morphology and have not been sufficiently studied are the solvent composition and the zone where the ZnO grows (i.e. within the bulk solution or on a substrate).

In this work, we study structure, morphology and optical emission of ZnO nanostructures obtained by solvothermal synthesis. We compare products from the bulk solution and on Si substrates and also study the role of adding methanol to the solvothermal solution. The methanol induces profound morphological changes, from nanorods to microprisms and eventually a porous film on Si. Both the methanol and the growth zone lead to strong effects on the optical emission from the ZnO structures.

## 2. Experimental Section

ZnO seeds were deposited on (100) Si substrates following the procedure previously reported [5]. Samples were synthesized by solvothermal synthesis in 25 mL polytetrafluoroethylene (PTFE) vessels within a stainless-steel autoclave, using zinc acetate dihydrate (CAS 5970-45-6, Alfa Aesar, >98%), HMTA (CAS 100-97-0, PanReac, > 99%) and three different solvent systems: water, water/methanol (1:1 ratio) and methanol (CAS 67-56-1, Cicarelli, 99.8%). For the synthesis, equimolar quantities

of both  $\text{Zn}^{2+}$  and HMTA ( $7.5 \times 10^{-4}$  mol) were added to the PTFE vessels, thus keeping the  $\text{Zn}^{2+}$ :HMTA ratio at 1:1. Then, the vessels were filled with the corresponding solvent (water, methanol or a mixture of both) until reaching 12.5 mL. The seeded substrates were put upside down into the PTFE vessels, the autoclaves were closed and heated for 4 h at 125 °C, then they were cooled down to room temperature. Two products were obtained from each reaction: i) ZnO powders that grew in the bulk solution zone (BSZ) and ii) ZnO on Si substrates (SiS). Previous to characterization, the BSZ samples were separated by centrifugation, washed with water/ethanol and dried on glass substrates at 125 °C. SiS samples were also washed with water/methanol and dried at 125 °C. Samples were studied by scanning electron microscopy, micro-Raman (532 nm wavelength, with 10 mW power) and photoluminescence measurements (325 nm line of a He-Cd laser at 15 mW power as the excitation source).

### 3. Results and discussion

Fig. 1(a-f) present SEM micrographs from all studied samples. When water was used as solvent, hexagonal nanorods were obtained for both SiS and BSZ samples [Fig. 1(a,d)]. When water/methanol mixture was used as solvent, hexagonal microprisms were obtained [Fig. 1(b,e)] and, in contrast to the case of water for which structures grew perpendicular to the substrate [Fig. 1(a)], here they grew in random directions. For the methanol case, a more drastic morphology change was observed: The BSZ powder consisted of nanoparticles [Fig. 1(c)], while the SiS sample exhibited a microporous thin film [see Fig. 1(f) and also Table 1, where sizes and aspect ratios of all structures are summarized].

The Raman spectra for samples studied are presented in Fig. 2. The non-polar  $E_2^{\text{low}}$  and  $E_2^{\text{high}}$  modes appear centered in the  $97.3\text{-}98.1\text{ cm}^{-1}$  and  $436.9\text{-}440.8\text{ cm}^{-1}$  ranges, respectively. The existence of these modes shows that samples crystallized in a

typical wurtzite crystalline phase and confirms the ZnO synthesis, even for pure methanol (for which the BSZ sample spectrum is only shown as for the SiS sample the Raman signal was too low to be detected).

Hence, the morphology of the obtained ZnO nanostructures can be strongly changed by incorporating methanol to the solvent. In particular, it is striking that nanorod formation is completely inhibited even while using HMTA, which is known to lead to elongated morphologies. Two different explanations have been proposed for the role of HMTA in promoting one dimensional growth. The first one assumes that HMTA is adsorbed on the nonpolar facets of the growing ZnO, acting as a capping agent that induces anisotropic growth along the polar *c*-axis direction [3,4]. The second explanation assumes that HMTA decomposes (to ammonia and formaldehyde) in the reactive medium, slowly releasing OH<sup>-</sup> ions and hence leading to slow ZnO growth under conditions near thermodynamic equilibrium (which also favor growth along the *c*-axis direction) [2]. The fact that solvothermal synthesis of ZnO nanorods without HMTA may also occur [6] indicates that indeed a capping agent is not needed for one dimensional growth. With zinc acetate dehydrate as the ZnO growth precursor, layered basic zinc (LBZ) salts are created as intermediate products:  $Zn_{1+x}(OH)_y(OCOCH_3)_z \cdot 2H_2O$  in aqueous solution [7] which changes to  $[Zn(MeOH)_{5-m}(MeO)_m(OCOCH_3)]^{1-m}$  in methanolic solution [8]. It has been shown that the specific LBZ morphology has an impact on the morphology of the ZnO products obtained during solution synthesis [9]. Hence, it may be expected that the addition of methanol to the solution leads to formation of new LBZ compounds which promote a new growth mechanism responsible for the modified ZnO morphologies observed here. However, there remains the question about the OH<sup>-</sup> source when pure methanol is used as the solvent. ZnO formation in alcoholic media without hydroxide additives has been rarely reported.

Hosono *et al.* obtained ZnO nanoparticles without hydroxides by using different alcohols as solvents, including methanol [10]. Their nanoparticles had sizes not greater than 10 nm (60 °C, 24 h of reaction); in contrast, we obtained nanoparticles with ~ 20 nm diameter (125 °C, 4 h, see Table 1) and a film on Si [Fig. 1(e, f)]. Hosono *et al.* argue that the LBZ compounds that form with methanol are hydrolyzed by H<sub>2</sub>O molecules from the zinc acetate dihydrate, followed by a condensation to form the nanoparticles. In our case, in addition to the zinc acetate dihydrate, the trapped atmospheric air molecules within the heated autoclaves, which are solubilized as a result of the thermal expansion of the reactive medium, should act as a supplementary source of H<sub>2</sub>O and O<sub>2</sub>.

Now we discuss the impact of the solvent composition on the PL from the ZnO structures obtained; spectra are shown in Fig. 3. All the samples exhibit the typically observed excitonic band in the UV and a broad band in the visible due to deep defect states. The following effects are observed:

1) For BSZ samples, the PL spectra have strong visible emission and a weaker UV band [Fig. 3(a)]. For the SiS samples [Fig. 3(c)], in contrast, the UV emission dominates the PL.

2) In both cases, the contribution from the visible emission increases at the expense of the UV emission when methanol is included in the solution, indicating the formation of additional defect states in the forbidden gap that act as luminescent centers, increasing the emission in the visible and reducing the contribution from competing excitonic recombination processes.

3) As seen in Fig. 3(b,d), for BSZ samples the UV band is broad with a maximum intensity at 3.15-3.18 eV and a marked shoulder at larger energy, while for SiS samples a narrower peak at 3.27-3.35 eV is observed. We believe the broad UV

band and shoulder for BSZ samples is related to the presence of mainly two different ZnO particles within the powders: a defected one with recombination processes involving traps leads to a dominant UV peak at a low energy and a low defect ZnO structure responsible for the shoulder at an energy position that resembles the narrower UV peak position observed for the SiS samples [Fig. 3(b,d)].

4) For pure methanol the UV band (for both BSZ and SiS) is clearly blueshifted. This effect is currently not understood and under study.

5) When fitting all the spectra with assumed Gaussian components [representative results in Fig. 3(e-f) and parameters in Table 1], we observe that the principal component in the visible for all studied samples is the yellow emission, which has been attributed to the oxygen vacancy [5]. This result indicates that effects on visible emission related with morphology, such as whispering gallery modes observed in ZnO with hexagonal cross section [11], do not have influence in these samples, since the visible emission has the same nature for hexagonal cross section nanowires and for spherical nanoparticles.

6) The dominant component in the BSZ sample is located close to 3.15 eV [Fig. 3(f)] and the difference with the first component at ~3.24 eV is too large to be associated with phonon replicas of excitonic emission [12]. This supports the assumption that the 3.15 eV peak is related to recombination processes through donor point defects [13].

#### 4. Conclusions

The methanol content in the solvent strongly affects the morphology and emission properties of ZnO grown by solvothermal synthesis, and inhibits the alkaline agent (HMTA) well-known role in producing well aligned ZnO nanorods on substrates.

The defect structure and optical emission properties of ZnO structures are strongly influenced by both the methanol content and the growth zone.

### Acknowledgment

This research was supported by SCAIT-UNT (PIUNT E637), CONICET (PIP 411) and ANPCyT (FONCyT – BID PICT 2015-0865).

### References

- [1] Djurišić AB, Chen X, Leung YH, Ng AMC, *J. Mater. Chem.* 2012;22:6526.
- [2] McPeak KM, Le TP, Britton NG, et al., *Langmuir* 2011;27:3672.
- [3] Saranya A, Devasena T, Sivaram H, Jayavel R, *Mater. Sci. Semicond. Process.* 2019;92:108.
- [4] Strano V, Urso RG, Scuderi M, et al., *J. Phys. Chem. C* 2014;118:28189.
- [5] González V, Marin O, Tirado M, Comedi D, *Mater. Res. Express* 2018;5:125003.
- [6] Sin JC, Lam SM, Lee KT, Mohamed AR, *Mater. Lett.* 2015;140:51.
- [7] Ku CH, Yang HH, Chen GR, Wu JJ, *Cryst. Growth Des.* 2008;8:283.
- [8] Hosono E, Fujihara S, Kimura T, Imai H, *J. Colloid Interface Sci.* 2004;272:391.
- [9] Morioka H, Tagaya H, Kadokawa JI, Chiba K, *J. Mater. Sci. Lett.* 1999;18:995.
- [10] Hosono E, Fujihara S, Kimura T, Imai H, *J. Sol-Gel Sci. Technol.* 2004;29:71.
- [11] Reimer T, Paulowicz I, Röder R, et al., *ACS Appl. Mater. Interfaces* 2014;6:7806.
- [12] Marin O, Alastuey P, Tosi E, et al., *Appl. Surf. Sci.* 2018;456:771.
- [13] Srokant V, Clarke DR, *J. Appl. Phys.* 1998;83:5447.



## Captions

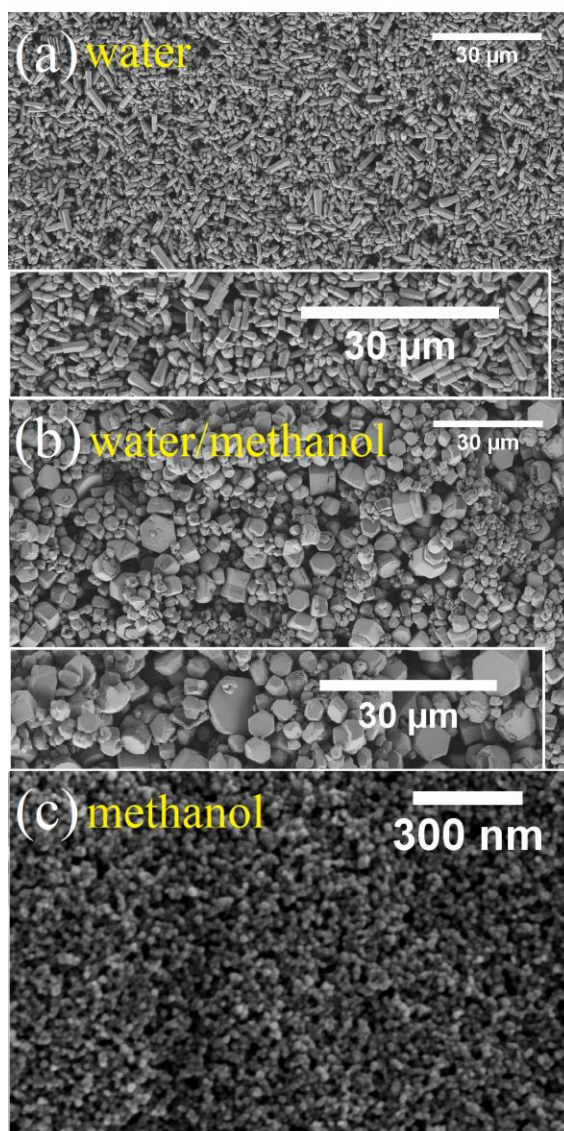
**Table 1.** Size parameters of the samples. W = water, MeOH = methanol; L, R, T = length, radius and thickness, respectively and energy of PL components from Gaussian fit.

**Figure 1.** SEM micrographs: (a,b and c) correspond to BSZ samples using water, water/methanol and methanol as solvent, respectively. (d, e and f) correspond to lateral and top views of SiS samples using water, water/methanol and methanol as solvent, respectively.

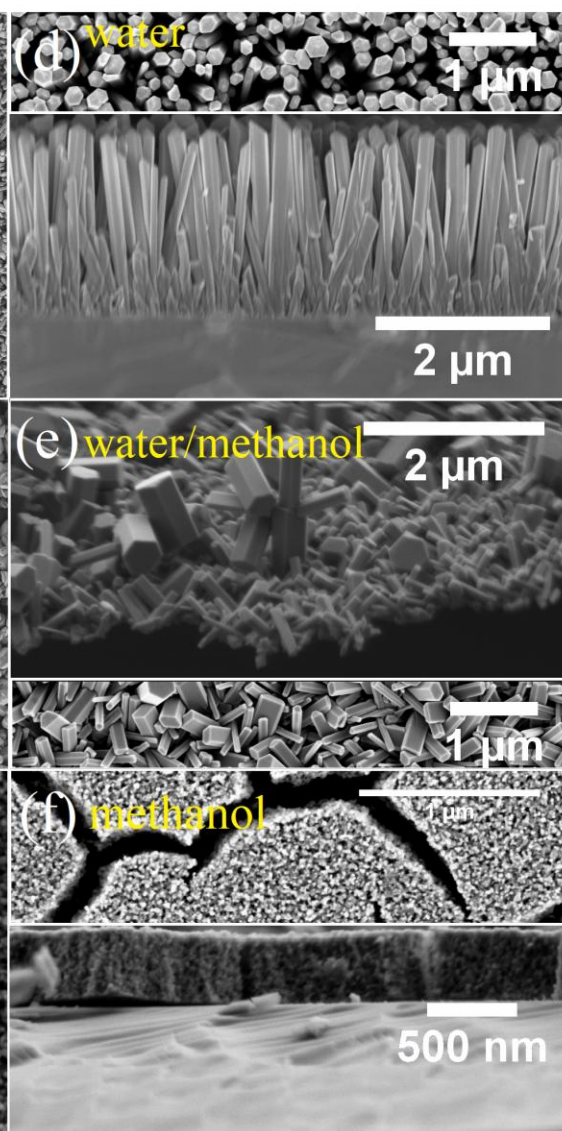
**Figure 2.** Raman spectra of samples.

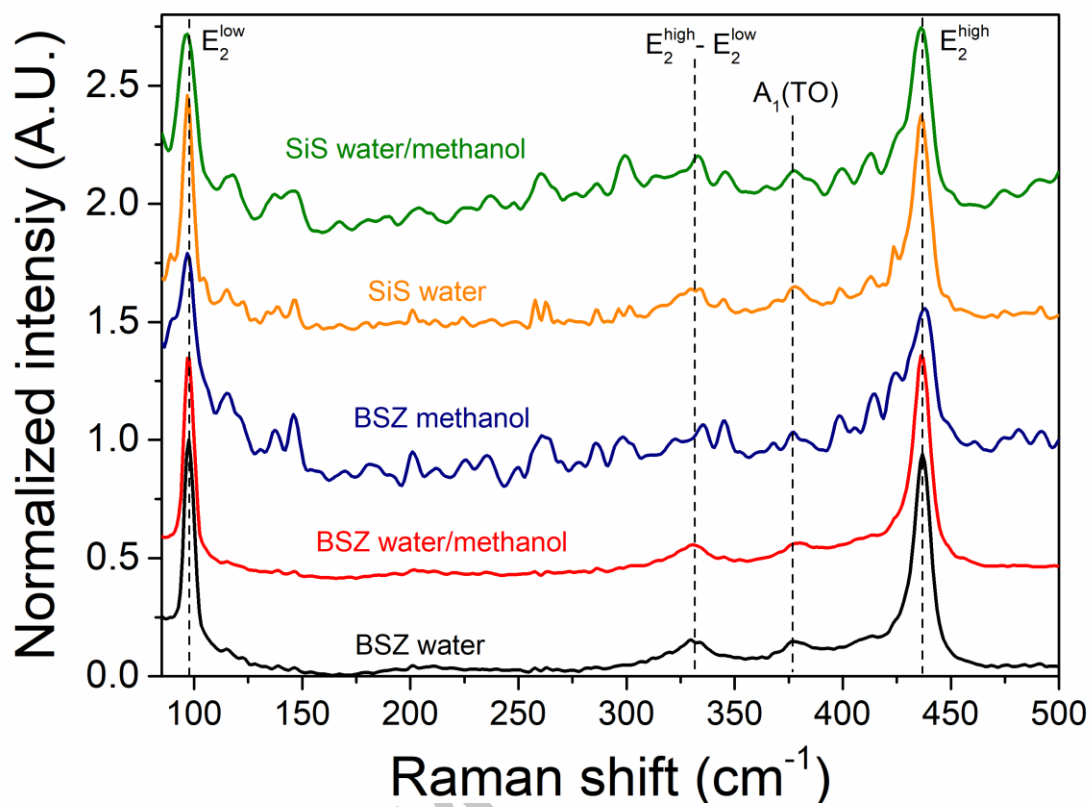
**Figure 3.** Normalized PL spectra of samples: (a) BSZ samples; (b) zoom on UV band region in (a) (renormalized); (c) SiS samples; (d) zoom of UV band region from (c); (e) visible emission from BSZ sample (water as solvent) and Gaussian fit components; (f) UV emission from BSZ sample (water as solvent) and Gaussian fit components.

ZnO samples grown at BSZ



ZnO samples grown on Silicon substrates





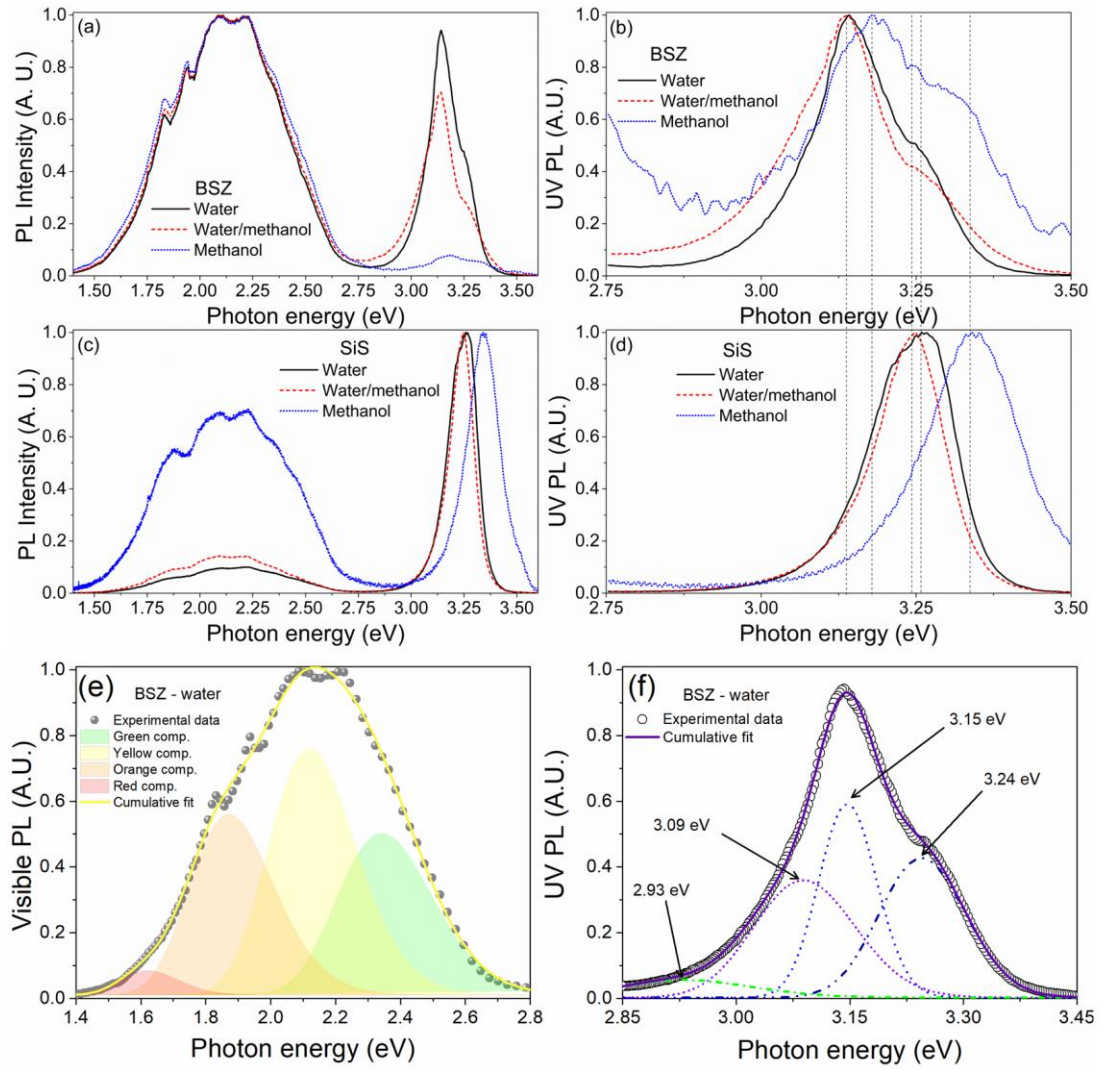


Table 1.

| Solvent |   | BSZ                       | SiS                       |                         | Aspect Ratio |      | Photoluminescence<br>UV peak position – Gaussian components (eV) |      |      |      |      |      |      |
|---------|---|---------------------------|---------------------------|-------------------------|--------------|------|--|------|------|------|------|------|------|
|         |   |                           |                           |                         | BSZ          | SiS  | BSZ  |      |      | SiS  |      |      |      |
| W       | L | $2.2 \pm 0.7 \mu\text{m}$ | $1.6 \pm 0.5 \mu\text{m}$ |                         | ~31          | ~21  | 3.24   | 3.15 | 3.09 | 2.92 | 3.28 | 3.20 | 3.11 |
|         | R | $70 \pm 10 \text{ nm}$    | $75 \pm 15 \text{ nm}$    |                         |              |      |  |      |      |      |      |      |      |
| W/MeOH  | L | $2.8 \pm 0.8 \mu\text{m}$ | $350 \pm 80 \text{ nm}$   |                         | ~1.4         | ~2.3 | 3.26   | 3.14 | 3.09 | 2.92 | 3.26 | 3.19 | 3.11 |
|         | R | $2 \pm 0.9 \mu\text{m}$   | $150 \pm 40 \text{ nm}$   |                         |              |      |  |      |      |      |      |      |      |
| MeOH    | R | $19 \pm 5 \text{ nm}$     | T                         | $380 \pm 10 \text{ nm}$ | -            | -    | 3.28   | 3.16 | 3.08 | 2.83 | 3.50 | 3.35 | 3.25 |
|         |   |                           | R                         | $22 \pm 5 \text{ nm}$   |              |      |  |      |      |      |      |      |      |

**Highlights**

- Methanol was added to solution during solvothermal synthesis of ZnO with HMTA
- ZnO products from the bulk solution were compared with ZnO grown on Si substrates
- ZnO morphology changed strongly as methanol was added to the solvothermal solution
- ZnO grown on Si substrate shows better optical emission than ZnO from bulk solution

ACCEPTED MANUSCRIPT

The authors declares that there is no conflict of interest regarding the publication of this article.

ACCEPTED MANUSCRIPT